

This is an Accepted Manuscript for *Journal of Glaciology*. Subject to change during the editing and production process.

DOI: 10.1017/jog.2024.94

Do atmospheric rivers trigger tabular iceberg calving?

Tristan RENDFREY,¹ Jeremy BASSIS,¹ Claire PETTERSEN,¹

¹*Department of Climate and Space Sciences and Engineering*

Corresponding author: <rendfrey@umich.edu>

ABSTRACT.

The processes governing iceberg calving from ice shelves remain poorly understood. Recent studies suggest that anomalous atmospheric moisture transport events—atmospheric rivers—can act as triggers for calving. These conclusions, however, were based on studies of case studies of individual icebergs or ice shelves, making it difficult to determine if this relationship remains apparent when considering a wider set of calving events and ice shelves. Here, we assemble an Antarctic-wide catalog of tabular iceberg calving events to evaluate whether a significant correlation exists between calving and enhancement of total and meridional integrated vapor transport (IVT), a measure of atmospheric moisture transport. We find that ~80% of the calving events in our study occur when metrics of IVT are less than the 90th percentile of their monthly climatologies. However, the remaining ~20% of calving events that occur during periods with short-term enhanced IVT exhibit a statistically significant correlation. The results, however, are regionally dependent, with a statistically significant correlation between enhanced IVT and calving in the Antarctic Peninsula and none in the Amundsen Sea Embayment. This suggests that, although enhanced IVT is not a primary control on the iceberg calving process, enhanced IVT may play a role in triggering calving events under certain conditions.

This is an Open Access article, distributed under the terms of the Creative Commons Attribution-NonCommercial-NoDerivatives licence (<http://creativecommons.org/licenses/by-nc-nd/4.0/>), which permits non-commercial re-use, distribution, and reproduction in any medium, provided the original work is unaltered and is properly cited. The written permission of Cambridge University Press must be obtained for commercial re-use or in order to create a derivative work.

25 INTRODUCTION

26 Freely floating ice shelves surround much of the Antarctic ice sheet, where they serve as the primary
27 sources of ice mass discharged into the ocean (Dupont and Alley, 2005). Antarctic ice shelves also provide
28 a buttressing stress on grounded ice (e.g., Dupont and Alley, 2005; Goldberg and others, 2009; Gagliardini
29 and others, 2010; Gudmundsson, 2013; Miles and others, 2022) that reduces mass flux across ice shelf
30 grounding lines. Buttressing from ice shelves therefore slows dynamic discharge from the Antarctic Ice
31 Sheet and stabilizes it from irreversible retreat associated with marine ice sheet and, potentially, marine
32 ice cliff instability (Bassis and Walker, 2011; Pollard and others, 2015; DeConto and Pollard, 2016; Edwards
33 and others, 2019; Garbe and others, 2020; Bassis and others, 2024).

34 Mass loss from ice shelves can decrease their ability to buttress upstream ice (Paolo and others, 2015;
35 Rignot and others, 2019). The process of mass loss from ice shelves is primarily controlled by a combination
36 of basal melting and iceberg calving (e.g., Liu and others, 2015). Observations currently show roughly equal
37 magnitudes of basal melt and iceberg calving contributions to the total mass loss from the entire Antarctic
38 Ice Sheet (e.g., Depoorter and others, 2013; Liu and others, 2015; Greene and others, 2022), although
39 the partition between the amount of mass lost to basal melt and calving is highly variable between ice
40 shelves (Liu and others, 2015; Davison and others, 2023). Currently, mass loss due to surface melt is small
41 over most Antarctic ice shelves (Kuipers Munneke and others, 2012; Lenaerts and others, 2019). However,
42 surface melt has been implicated in the hydrofracture-related explosive collapse of the Larsen B ice shelf,
43 which occurred unexpectedly in 2002 following a period of melt pond formation (van den Broeke, 2005;
44 Glasser and Scambos, 2008; Banwell and others, 2013).

45 Although surface and basal melting are directly controlled by both atmospheric and oceanic forcing,
46 the overall processes controlling iceberg calving remain poorly understood (e.g., Lazzara and others, 1999;
47 Walker and others, 2015, 2021; Benn and others, 2022; Alley and others, 2023; Bassis and others, 2024).
48 Unlike the spectacular disintegration of the Larsen B ice shelf, the calving process from most ice shelves
49 occurs through the initiation and propagation of rifts—fractures that penetrate the entire ice shelf thickness,
50 which can propagate on time scales up to decades (e.g., Bassis and others, 2008; Walker and others, 2013;
51 Lipovsky, 2020). Rift-propagating processes contribute to the calving of tabular icebergs when they result
52 in the separation of an area of ice from the rest of the shelf (Lazzara and others, 1999; Joughin and
53 MacAyeal, 2005; Kenneally and Hughes, 2006; Indrigo and others, 2020). Tabular icebergs, which can

54 exceed hundreds of kilometers in length, remove mass near-instantaneously from the Antarctic Ice Sheet
55 (Lazzara and others, 1999; Joughin and MacAyeal, 2005) and are the primary mode of calving from ice
56 shelves (Fricker and others, 2002; Bassis and others, 2008, 2024).

57 The tabular iceberg calving process has traditionally been thought to be primarily controlled by the
58 internal stress within the ice shelves (Robin, 1979; Bassis and others, 2008; Amundson and Truffer, 2010;
59 Humbert and Steinhage, 2011; Bassis and Jacobs, 2013; Walker and others, 2015; Indrigo and others, 2020).
60 However, studies have also indicated external stress from tidally-induced currents (Legrésy and others,
61 2004; Lescarmontier and others, 2015) and pulses of ocean swell (MacAyeal and others, 2006; Bromirski
62 and others, 2010; Sergienko, 2010) as triggers for calving. Alternatively, unusually large sea surface slopes
63 have also been hypothesized to induce rift propagation on Antarctic ice shelves (Mayet and others, 2013;
64 Francis and others, 2021). However, the physical connection between these environmental triggers can be
65 difficult to identify, as Bassis and others (2008) demonstrated that the stresses imposed on the ice are
66 associated with many of these environmental forcings is much smaller than the internal stresses within the
67 ice.

68 Recently, tabular iceberg calving events from the Larsen A, B and C ice shelves, the Amery Ice Shelf,
69 the Brunt Ice Shelf, and the Conger Ice Shelf have been linked to unusually strong poleward atmospheric
70 moisture transport (i.e., atmospheric rivers; Francis and others (2021, 2022); Laffin and others (2022);
71 Wille and others (2022, 2024)). In particular, Wille and others (2022) found that 60% of calving events
72 from the Larsen A, B, and C ice shelves were triggered by atmospheric rivers. It is, however, unclear
73 if these findings generalize to other ice shelves in other regions. These atmospheric moisture transport
74 extremes also correlate with many other potential triggers, including sea ice clearing and large sea surface
75 slopes (Massom and others, 2018; Dziak and others, 2019; Francis and others, 2021, 2022; Wille and others,
76 2022, 2024). Moreover, the warm and moist atmospheric conditions and radiative effects associated with
77 atmospheric rivers are directly related to surface meltwater formation on the ice shelves, which could make
78 ice shelves more vulnerable to hydrofracture-induced collapse (Turton and others, 2020; Laffin and others,
79 2022; Wille and others, 2022; Clem and others, 2022).

80 Determining the potential relationship between the timing of iceberg calving events and enhanced atmo-
81 spheric moisture transport, however, remains challenging. Although some calving events may coincide with
82 elevated atmospheric integrated vapor transport, it is possible that this relationship is spurious, resulting in
83 false correlations. This is especially true for regions where enhanced atmospheric moisture intrusions occur

84 relatively often compared to the frequency of calving events. Moreover, although studies of individual ice
85 shelves can avoid some of the issues around false attribution, they may not reveal heterogeneous behavior
86 of ice shelves in different glaciological or climatological regimes. For example, the Antarctic Peninsula is lo-
87 cated relatively far North compared to the Amundsen Sea Embayment, with some ice shelves experiencing
88 surface melt (van den Broeke, 2005; Kuipers Munneke and others, 2018). By contrast, the Amundsen Sea
89 Embayment ice shelves are located in regions with cold atmospheric conditions compared to the Antarc-
90 tic Peninsula and experience little surface melt (Trusel and others, 2013). Both the Antarctic Peninsula
91 and Amundsen Sea ice shelves, however, are located in regions where previous studies have documented
92 synoptic-scale conditions that favor enhanced moisture transport (Nicolas and Bromwich, 2011; Wille and
93 others, 2021; Swetha Chittella and others, 2022). Studies further provide evidence that elevated atmo-
94 spheric moisture transport might trigger calving from the Antarctic Peninsula (Laffin and others, 2022;
95 Wille and others, 2022).

96 Here, we seek to expand upon results from previous case studies and work focused on calving from the
97 Antarctic Peninsula by examining if links between enhanced moisture transport and calving hold across
98 a broader set of events from all Antarctic ice shelves. We use this extended dataset to see if there are
99 regional differences in sensitivity to atmospheric moisture transport, and to determine when atmospheric
100 moisture transport exhibits a statistically significant correlation with the timing of iceberg calving.

101 DATA AND METHODS

102 We first constructed a catalog of iceberg calving events, focusing on large “tabular” icebergs with a charac-
103 teristic length much larger than the ice thickness (e.g., Lazzara and others, 1999; Budge and Long, 2018).
104 We then examined the monthly climatology of total and meridional moisture transport over each Antarctic
105 ice shelf with a tabular iceberg calving event. This monthly climatology allowed us to assess the number
106 of calving events that were preceded by enhanced moisture transport over each individual shelf. Finally,
107 we tested if the relationship between enhanced moisture transport and the timing of iceberg calving is
108 statistically significant using a bootstrap (Efron, 1979). We describe each step in this process in more
109 detail below.

110 **Catalog of tabular iceberg calving events**

111 *US National Ice Center Named Tabular Icebergs*

112 To construct our catalog of tabular iceberg calving events, we used the US National Ice Center (USNIC;
113 usicecenter.gov) press releases. These press releases document new icebergs, including the location of where
114 the new iceberg was first sighted, as well as the date of first sighting, the size, and the ice shelf from which
115 the iceberg detached. We use USNIC press releases that document all icebergs sighted between November
116 2013 and December 2023 with a longest side length greater than 7 nautical miles or a total area greater
117 than 20 nautical miles squared (<https://usicecenter.gov/Products/AntarcIcebergs>). This detection method
118 excludes the many smaller icebergs that can detach from ice shelves and glaciers, allowing us to focus on
119 the processes governing the detachment of large tabular icebergs that feature prominently in the calving
120 cycle of most ice shelves (Alley and others, 2023; Bassis and others, 2024).

121 *MODIS image analysis of calving event timing*

122 Determining the timing of iceberg calving required more information than we could attain from the USNIC
123 press releases alone, both because they are issued after a calving event occurs and the reported timing of
124 iceberg detachment is limited by the weekly timing of press releases. To more precisely identify the
125 timing of iceberg detachment, we additionally examined satellite images from the Moderate Resolution
126 Imaging Spectroradiometer (MODIS) instrument. We accessed images of iceberg calving viewed by the
127 MODIS instruments from the Aqua and Terra satellites (Xiong and Barnes, 2006) using NASA WorldView
128 (worldview.earthdata.nasa.gov). The Aqua and Terra satellites view the same point on Earth roughly three
129 hours apart (Crosson and others, 2012), therefore we had two images available for each day from 2013–23.
130 MODIS visible images have been previously used to determine calving event timing (e.g. Wille and others,
131 2022). Here, we examined MODIS images using the true-color visible imagery (0.45–0.67 μm wavelength;
132 500 m spatial resolution) during seasons with available sunlight (approximately October through April) over
133 the iceberg or ice shelf. For seasons without sufficient sunlight (approximately April through October), we
134 used the MODIS infrared channels (10.780–11.280 μm wavelength) to distinguish between the ice shelves,
135 icebergs, and ocean. The MODIS infrared brightness temperatures allow for detection of the icebergs, but
136 have lower spatial resolution than the visible channels (1 km). However, because we were only focused
137 on tabular icebergs that are much larger in size than 1 km^2 , the lower resolution in the infrared does not

138 affect our ability to detect iceberg calving detachment events.

139 We determined the timing of iceberg calving by combining the information from MODIS and USNIC
140 press releases in the following way, illustrated in Figure 1: We first examined the USNIC press release
141 (Figure 1a) for a date and the location to begin viewing the MODIS visible and/or infrared images over
142 the iceberg (Figure 1b). We then obtained the MODIS imagery of the same scene for the previous day, and
143 re-centered the image on the iceberg to account for drift in the open ocean waters (e.g. Figure 1c). We
144 repeated this process, stepping back one day and re-centering the image on the iceberg (e.g., Figure 1d),
145 until the iceberg appears to be attached to an ice shelf (Figure 1e). We identified the first day of images
146 that show the detachment of the iceberg from the shelf as the “calving event” and the day of the image as
147 the time of the event. An important caveat to our method is that our catalog was determined using the
148 date when icebergs start to drift away from their parent ice shelf, which may occur after some time after
149 rifts first isolate an iceberg, especially if icebergs are surrounded by fast ice or *mélange* (e.g., Schlemm and
150 Levermann, 2021; Alley and others, 2023). Cloudy conditions may also obscure the view of the ice surface
151 in both visible and infrared images. This introduced an uncertainty in the calving event timing that is
152 equal to the number of days in a cloudy period during iceberg detachment. This uncertainty was less than
153 two days for 29 of the 41 events (70% of the calving events) and up to five days for 12 of the events (30%
154 of the calving events).

155 *Catalog of tabular iceberg calving events*

156 To focus on the atmospheric drivers of calving, we removed icebergs from our catalog that formed through
157 fragmentation or fracture of existing floating icebergs (e.g. England and others, 2020). For the same reason,
158 we also removed the entries for icebergs that detached due to collisions between ice shelves and already-
159 floating icebergs. This removed two iceberg detachments. Additionally, following previous case studies
160 that argued that the cumulative effect of moisture transport was the trigger for calving (e.g., Francis and
161 others, 2021, 2022), we then examined running averages of atmospheric variables over 7 and 28 days prior
162 to each calving event (see next section for details). Consequently, if an iceberg calved from the same ice
163 shelf in the 28 days prior to an identified event, we removed the iceberg that calved later from the catalog
164 to preserve the independence of the 28 day running average. This method removed one iceberg from the
165 Conger ice shelf (C-38) and one from Pine Island ice shelf (B-36) from the catalog. Finally, if multiple
166 icebergs detach from the same ice shelf on the same day, we consider them as a single calving event. We

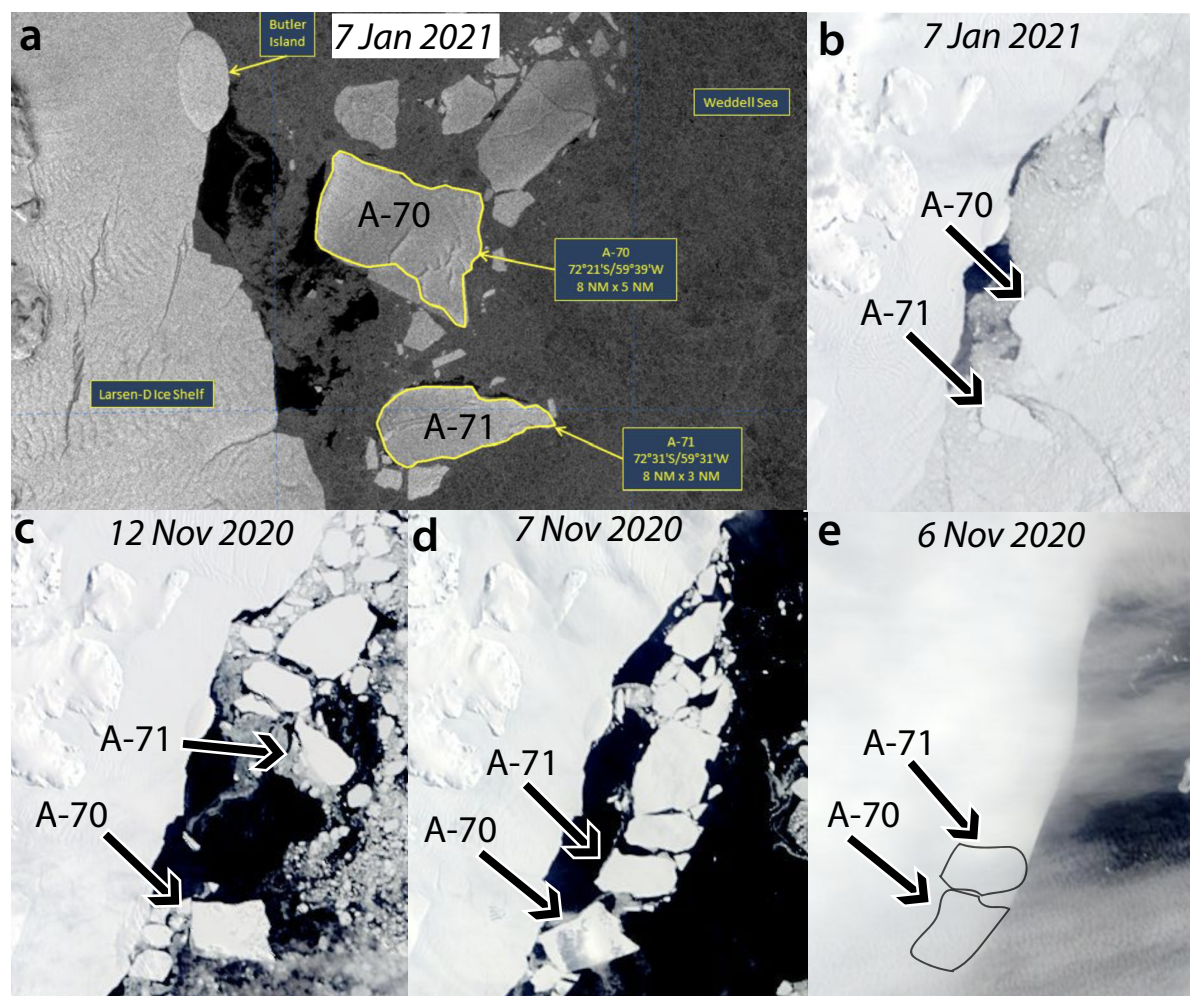


Fig. 1. An example of the process used to determine iceberg calving dates. (a) Example showing an image of icebergs A-70 and A-71 from 7 January 2021 provided by the USNIC press release for the icebergs issued on 8 January. (b) The same scene viewed by MODIS, including the Larsen D ice shelf. (c) MODIS image of the Larsen D ice shelf on 12 November 2020, 8 days before calving, which was used as part of the sequence that tracked the icebergs from 7 January 2021 back to the calving date. (d) MODIS image on day of calving iceberg A-70 and A-71 (and smaller unnamed icebergs). (e) MODIS image of the ice shelf one day prior to the calving event. In this panel, indications of the outlines of the ice shelf areas that will calve into icebergs A-70 and A-71 are shown.

167 made these decisions to avoid the potential to overestimate the influence of atmospheric drivers if multiple
168 calving events are correlated with the same atmospheric event. We found that the statistical significance
169 of our results, however, was insensitive to these omissions.

170 Our final catalog included 41 tabular iceberg calving events over a total of 23 ice shelves. We noted
171 that 13 calving events came from ice shelves located in the Amundsen Sea Embayment (defined as the Pine
172 Island, Thwaites, Dotson, and Getz ice shelves), and 8 calving events came from Antarctic Peninsula ice
173 shelves (defined as the Larsen C, D, F, and George VI ice shelves).

174 **Atmospheric moisture transport analysis over Antarctic ice shelves**

175 *ERA5 reanalysis*

176 To assess atmospheric moisture transport over Antarctic ice shelves prior to the calving events in our cat-
177 alog, we examined variables using the ECMWF fifth generation atmospheric reanalysis (ERA5; Hersbach
178 and others (2020)). ERA5 has a spatial grid of 0.25° resolution, and we used a 3-hourly temporal resolu-
179 tion. We focused here on the vertically integrated moisture transport (IVT), a common measure used to
180 quantify moisture transport. IVT measures the flux of water vapor through a column of the atmosphere,
181 which depends on the water vapor content of and wind speed through the column. IVT therefore can be
182 expressed in units of $\text{kg m}^{-1} \text{s}^{-1}$. Very high values of IVT in a narrow enough region are traditionally used
183 to characterize atmospheric rivers (e.g. Gimeno and others, 2014; Wille and others, 2019). Because atmo-
184 spheric moisture originates in the tropics and is then transported poleward, atmospheric river detection has
185 often focused on the intensity of poleward-directed IVT (the meridional component of IVT, (e.g. Wille and
186 others, 2019). The zonal component describes easterly or westerly-directed IVT, and accounts for moisture
187 transport events that are not purely in the poleward direction. Some studies (e.g. Bozkurt and others,
188 2022) use total IVT, which is equal to the magnitude of the IVT vector and is calculated from the sum
189 of the squares of the zonal and meridional components of IVT. To account for the different definitions, we
190 adopt both metrics of IVT to investigate the influence of water vapor transport on iceberg calving from ice
191 shelves. We calculate the total IVT from the zonal (IVT^{U}) and meridional components of the IVT vector
192 (IVT^{V}), both obtained from the ERA5 reanalysis. We calculated the total IVT, or the magnitude of the
193 IVT vector (denoted IVT^{T}) from the components according to $\text{IVT}^{\text{T}} = \sqrt{(\text{IVT}^{\text{U}})^2 + (\text{IVT}^{\text{V}})^2}$. In addition
194 to IVT^{T} , we examined IVT^{V} , which is linked to the strength of moisture transport across the midlatitudes
195 towards the polar regions, both poleward and equatorward (Bozkurt and others, 2018; Nash and others,

196 2018; Shields and others, 2022). Both IVT^T and IVT^V have been used to characterize atmospheric rivers
197 over Antarctica (e.g., Gorodetskaya and others, 2014; Terpstra and others, 2021; Wille and others, 2021;
198 Adusumilli and others, 2021; Gorodetskaya and others, 2023; Maclennan and others, 2023; Rendfrey and
199 others, 2024).

200 *Averaging IVT over ice shelves bounds*

201 To evaluate the atmospheric moisture transport conditions over the ice shelves preceding calving events,
202 we used the ice shelf bounds from Mouginot (2017) for the ice shelves in our catalog. Changes in ice
203 shelf area from the years 2007—2009 included in the study of Mouginot (2017) are relatively small for ice
204 shelves included in our study and do not affect the ERA5 points included in the ice shelf bounds. We
205 then computed the spatial average of total IVT (IVT^T) and the meridional IVT (IVT^V) for every 3-hour
206 time step available in the ERA5 data. To do this, we selected the ERA5 grid points that are contained
207 within each ice shelf's respective boundary (Figure 2a). We then used those grid points to compute the
208 spatial average of IVT^T and IVT^V over each ice shelf. Because there is a large range of sizes among the ice
209 shelves, the number of ERA grid points per ice shelf varies. The latitudes and longitudes corresponding to
210 the ERA5 grid points used for each ice shelf are given in Excel Table S2 in the Supplementary Material.

211 *Short-term and long-term temporal IVT averages*

212 We next calculated 7- and 28-day running averages of the variables for each 3 hour time step in the ERA5
213 climatology after we averaged the variables spatially within the ice-shelf bounds. We chose the 7-day rolling
214 mean for each ice shelf as a “short-term” time scale to align with the 5-day cumulative IVT analyzed by
215 Wille and others (2022); however, we included two additional days to account for the uncertainty in our
216 calving event date estimation methodology. We chose a 28-day rolling mean for the “long-term” influence
217 based on case studies of iceberg calving from the Brunt and Amery ice shelves (e.g. Francis and others,
218 2021, 2022). We denote the 28-day running average of IVT^T and IVT^V with the variables IVT_{28}^T and
219 IVT_{28}^V , respectively. Similarly, we denote the 7-day running average of IVT^T and IVT^V with the variables
220 IVT_7^T and IVT_7^V (see Figure 2b for an example of IVT_7^T before a calving event). We also analyzed 14
221 day running averages, but results from the 14 day averages were similar to the 7 and 28 day and did not
222 provide additional insight. We generally refer to the results of these computations, IVT_{28}^T , IVT_7^T , IVT_{28}^V ,
223 and IVT_7^V , as the metrics of IVT. We also more specifically refer to IVT_{28}^T and IVT_{28}^V jointly as the 28-day

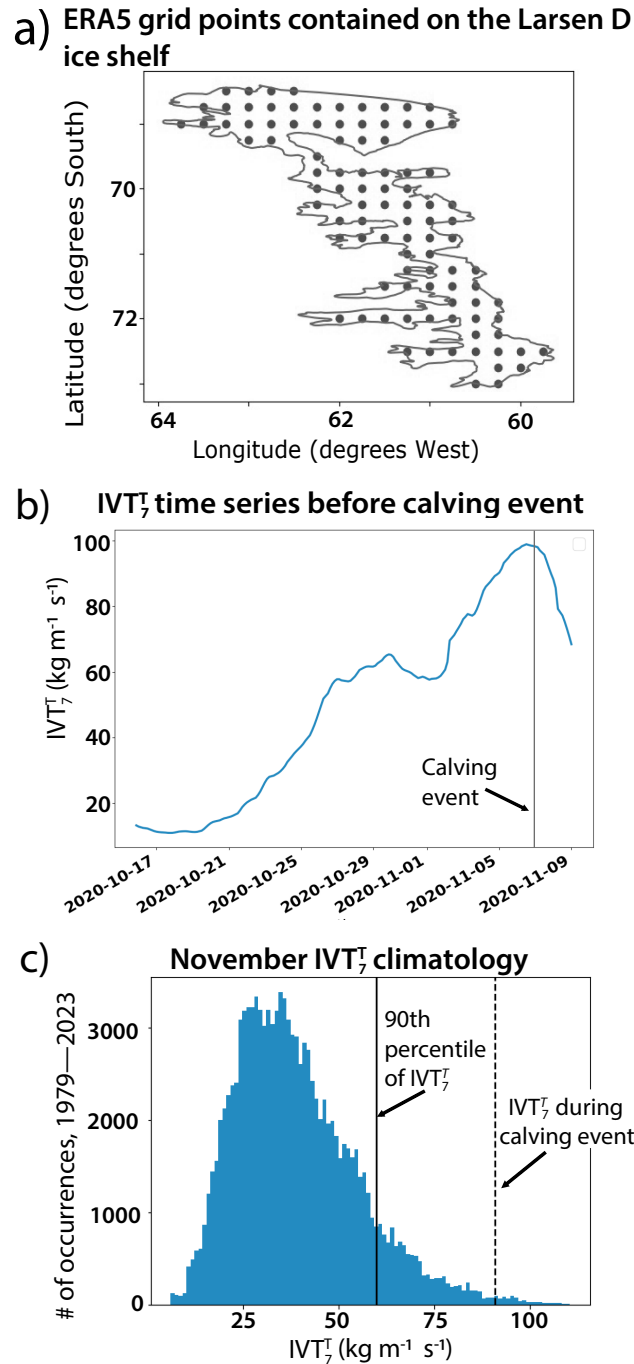


Fig. 2. Steps of the described method displayed graphically for the 7 November 2020 calving event from Larsen D as an example. (a) ERA5 grid point selection within the bounds of the Larsen D ice shelf. (b) A time series of IVT_7^T prior to the example calving event. (c) An example of the November climatology of IVT_7^T from 1979–2023 for the Larsen D ice shelf. Y-axis values correspond to the number of occurrences for each binned value of IVT_7^T in November months between 1979–2023. Vertical lines show the 90th percentile of the November IVT_7^T distribution for 1979–2023 and the value of IVT_7^T for the example calving event.

224 metrics of IVT, and likewise the IVT_7^T and IVT_7^V as the 7-day metrics of IVT.

225 **Statistical significance of correlations**

226 *Climatology and definition of enhanced IVT*

227 We first determined the climatology of our 4 metrics of IVT over as long of a period available from the ERA5
228 reanalysis, which is between the years 1979 and 2023. The climatologies were computed independently for
229 each ice shelf and for each month. Because IVT does not follow a normal distribution, we created histograms
230 of the metrics of IVT for each of the monthly climatologies for each ice shelf. We used monthly climatology
231 to be consistent with previous studies (e.g. Wille and others, 2022, 2024). It is possible to instead determine
232 extreme events based on the annual climatology. This results in fewer calving events that are identified as
233 coincident with extreme IVT and reduces the statistical significance of the association. We then defined
234 “enhanced IVT” with respect to each of our 4 metrics of IVT (IVT_{28}^T , IVT_7^T , IVT_{28}^V , and IVT_7^V) as any
235 value that exceeded the 90th percentile of the monthly climatology for each ice shelf (Camuffo and others,
236 2020) (an example of an event with enhanced IVT_7^T is illustrated in Figure 2c). We then counted the
237 number of calving events in the catalog that have enhanced IVT for the four metrics for each ice shelf
238 (IVT_{28}^T , IVT_7^T , IVT_{28}^V , and IVT_7^V).

239 *Estimating the statistical significance between IVT and calving events*

240 To test the possibility that the timing between calving events and IVT is coincidental, we performed a
241 bootstrap analysis (Efron, 1979). The bootstrap seeks to determine the probability that enhanced metrics
242 of IVT are associated with calving events simply by random chance. We estimated this probability as
243 follows: for each calving event in our catalog, we used a random number generator to choose a date from
244 the same month and ice shelf location as the observed calving event between the years 1979 and 2023.
245 We called this a “synthetic event”. One iteration of this process produces 41 synthetic events drawn from
246 the same ice shelves (and months) as the observed set of calving events. We then computed the 4 metrics
247 of IVT for each synthetic event in the synthetic set to determine which (if any) of our metrics for IVT
248 are enhanced. This provides a synthetic catalog of calving events where a fraction of the synthetic calving
249 events are associated with one or more of our metrics for enhanced IVT purely by chance. We then repeated
250 this process for 10,000 iterations to produce 10,000 sets of 41 synthetic events.

251 To estimate the probability that the observed association occurred purely by chance, we compared the

252 number of observed calving events with enhanced metrics of IVT against the fraction of our synthetic sets
253 that contained an equal or greater number of synthetic calving events with enhanced metrics of IVT. We
254 did this calculation separately for each of our four metrics of IVT. For example, if our catalog had 10 calving
255 events and 3 of those calving events were associated with enhanced IVT_7^V , we would calculate the fraction
256 of synthetic sets that have 3 or more calving events with enhanced IVT_7^V . If the fraction of synthetic
257 events was, say, 20%, then there is a 20% chance that the 3 events observed were associated with enhanced
258 IVT_7^V by random chance alone. We defined statistical significance using the standard 95% confidence
259 interval (Wilks, 2011). Hence, we considered the relationship between enhanced IVT and the timing of
260 calving events to be statistically significant if an equal or greater number of synthetic events associated
261 with enhanced metrics of IVT than calving events occurs in 5% or fewer of our 10,000 iterations. An
262 important caveat is that our bootstrap assumed metrics of IVT could be treated as stationary stochastic
263 processes. If climate change has led to more frequent or more intense moisture transport in more recent
264 decades, as some studies suggest (e.g., Espinoza and others, 2018; Payne and others, 2020), our bootstrap
265 could slightly overstate the significance of enhanced IVT.

266 **Study regions**

267 We applied our bootstrap to the entire, Antarctic-wide, catalog of calving events. However, given the
268 different glaciological and climatological environments experienced by ice shelves across the Antarctic
269 Ice Sheet, it is possible that certain regions—or ice shelves—are more sensitive to enhanced moisture
270 transport than others. For this reason, we also performed the bootstrap for calving events in two regions
271 of interest: the Amundsen Sea Embayment and Antarctic Peninsula. Ice shelves in these two regions
272 have sufficient calving events for regional statistics, but also experience climate forcing from both the
273 ocean and atmosphere. The Amundsen Sea Embayment experiences colder atmospheric conditions in its
274 southerly location (Rignot, 2002; Trusel and others, 2013), while the more northerly Antarctic Peninsula
275 ice shelves experience warmer near-surface air temperatures, which can cause widespread surface melt
276 (Kuipers Munneke and others, 2018; Costi and others, 2018).

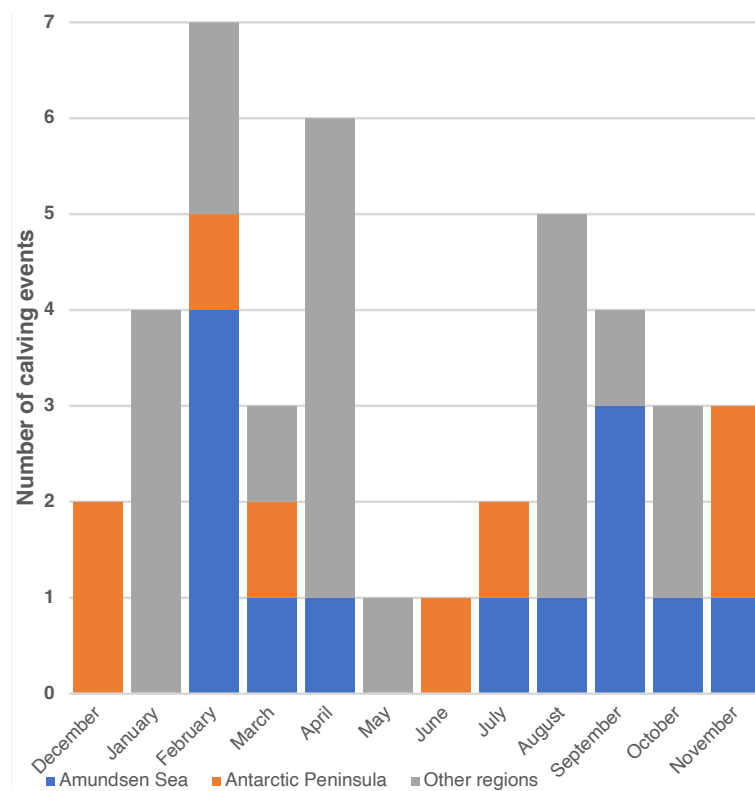


Fig. 3. The number of calving events in the catalog in each month. The number of calving events in the Amundsen Sea Embayment (in orange) and Antarctic Peninsula (in blue) are presented along with the number of calving events from all other regions of Antarctica (in grey).

277 RESULTS

278 Iceberg calving event timing

279 Our catalog of tabular calving events includes 41 events from 23 ice shelves. Calving events occurred
280 during each month of the year and from different portions of the Antarctic Ice Sheet (Figure 3). The
281 largest number of events occurred during Austral summer (14 in December, January, February), whereas
282 the fewest occurred during Austral winter (5 in June, July, August). We see 9 events during March, April,
283 and May and 10 events during September, October, November. The majority of ice shelves in our catalog
284 experienced two or fewer calving events; only the Pine Island (7 events), Larsen D (5 events), Getz (4
285 events), and Ninnis (3 events) ice shelves experienced more than two events. The tabular icebergs in our
286 catalog range in size from approximately 70 km² up to 7,000 km² in surface area at the time of calving.
287 Excel Table S1 in the Supplementary Material contains the calving dates, their respective ice shelves, the
288 size of the icebergs, and the location of the iceberg at detection, as well as a link to the original USNIC
289 press report.

290 Are calving events associated with enhanced values of 28-day IVT?

291 We first examined the two 28-day metrics of IVT (IVT_{28}^T and IVT_{28}^V) to determine if the timing of the
292 calving events in our catalog are associated with longer-term synoptic scale forcing from IVT. Figure 4
293 shows the fraction of calving events from each ice shelf that are coincident with enhanced 28-day metrics
294 of IVT. We find that 35 of the 41 (85%) calving events occurred during times when neither 28-day metric
295 of IVT was enhanced. Conversely, we find that, for both IVT_{28}^T and IVT_{28}^V , 6 out of the 41 (15%) calving
296 events did occur when the metrics of IVT were enhanced. The calving events with enhanced 28-day are
297 primarily located at the Larsen D, Getz, Pine Island, Vigrid and Baudouin ice shelves. However, despite
298 the similarity in total numbers of events associated with the enhanced 28-day metrics of IVT, there are
299 slight differences in the calving events that are identified as being associated with enhanced IVT_{28}^T and
300 IVT_{28}^V . For example, the calving event from the Baudouin ice shelf is associated with enhanced IVT_{28}^V , but
301 not IVT_{28}^T whereas, the calving event from the Vigrid ice shelf has enhanced IVT_{28}^V , but not IVT_{28}^T . This
302 indicates that there is some sensitivity in our results to the metrics used.

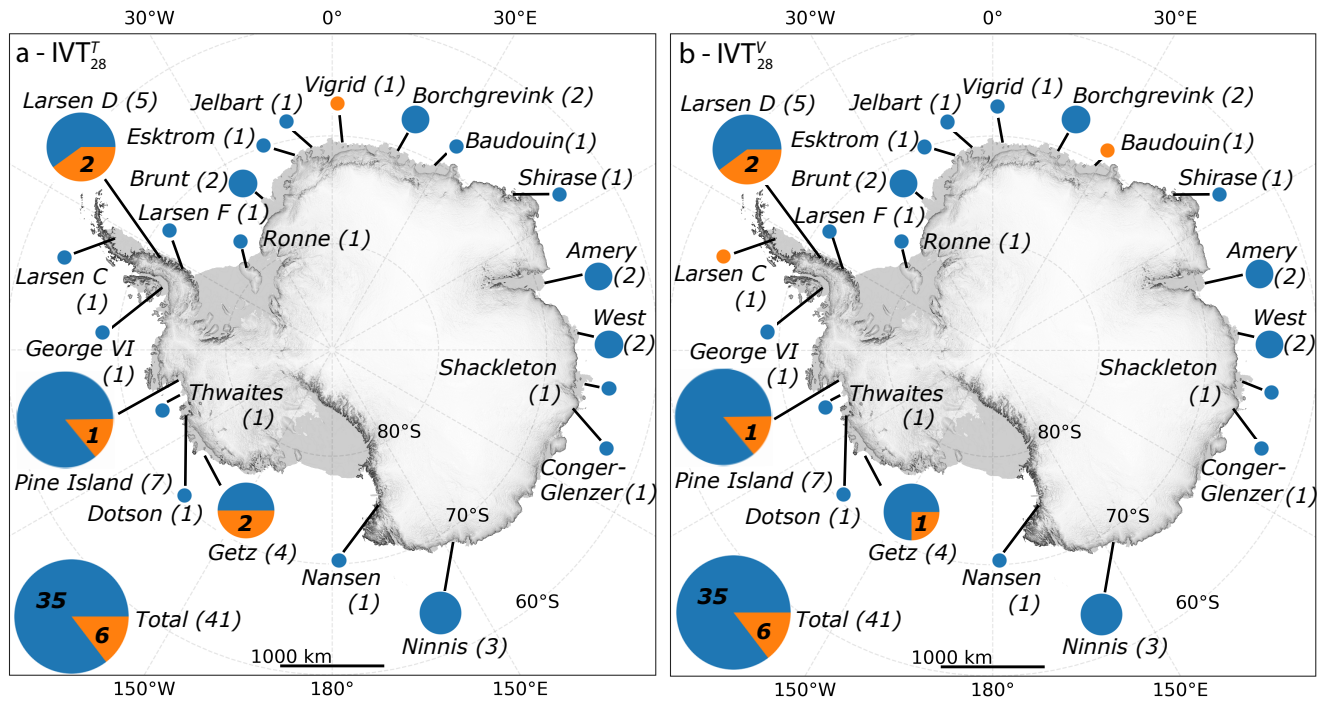


Fig. 4. Calving events per ice shelf with the fraction of events that have enhanced 28 day IVT, shaded in orange, for (a) total IVT magnitude, IVT_{28}^T , and (b) meridional IVT, IVT_{28}^V . The radius of each circle is proportionate to the total number of calving events from the ice shelf associated with it. The total number of calving events from each ice shelf is listed beside the label for each circle. The numbers in each orange region are the counts of events with enhanced IVT_{28}^T or IVT_{28}^V . The total number of calving events is shown boxed in the lower left corner.

303 Are calving events associated with enhanced 7-day IVT?

304 We next analyzed the relationship between calving and enhanced IVT_7^T and IVT_7^V (Figure 5). Similar to
305 the 28-day metrics of IVT, the majority of calving events are not associated with enhanced 7-day metrics
306 of IVT (32 out of 41 or 78%). However, we see a larger number of calving events that are associated with
307 enhanced 7-day metrics of IVT (9 out of 41) compared to the 28-day metrics of IVT (6 out of 41). We
308 again see slight differences between the calving events associated with enhanced 7-day metrics of IVT.
309 Here, the Larsen C and Ninnis Ice Shelves have calving events associated with enhanced IVT_7^V , but not
310 IVT_7^T , whereas the Ekstrom and George VI ice shelves had a calving event associated with enhanced IVT_7^T ,
311 but not IVT_7^V . Overall, the ice shelves that had calving events associated with enhanced IVT_7^T or IVT_7^V
312 are similar to those that had calving events associated with enhanced IVT_7^T or IVT_7^V , with the exception
313 of calving events from the Ekstrom and Amery Ice Shelves that are associated with enhanced 7-day but
314 not 28-day IVT. Hence, the 7-day metrics of IVT results in more calving events associated with enhanced
315 IVT from a larger number of ice shelves than the 28-day metrics of IVT.

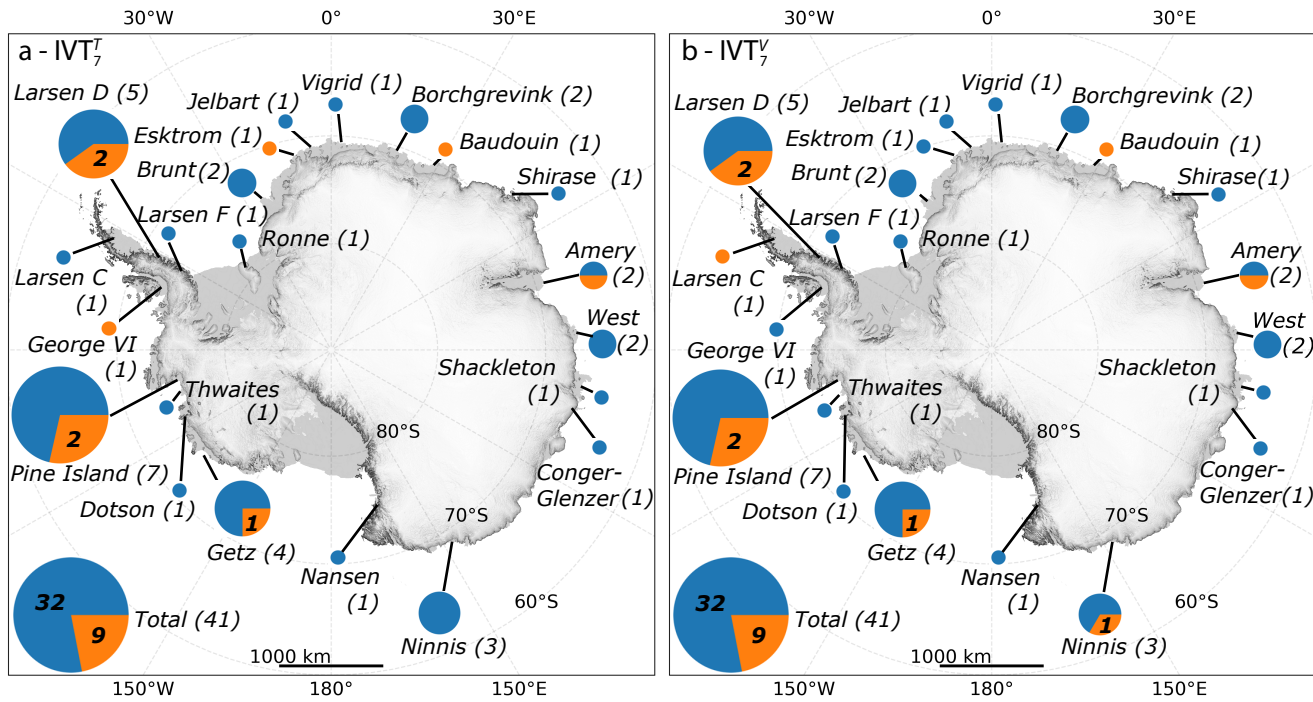


Fig. 5. Calving events per ice shelf with the fraction of events that have enhanced 7 day IVT, shaded in orange, for (a) total IVT magnitude, IVT_7^T , and (b) meridional IVT, IVT_7^V . The radius of each circle is proportionate to the total number of calving events from the ice shelf associated with it. The total number of calving events from each ice shelf is listed beside the label for each circle. The numbers in each orange region are the counts of events with enhanced IVT_7^T or IVT_7^V . The total number of calving events is shown boxed in the lower left corner.

316 **Is the association between enhanced IVT and calving events statistically significant?**

317 Despite the fact that most calving events are not associated with enhanced values of any of our four metrics
318 of IVT, we do find that 6 or 9 of the 41 calving events are correlated with one or more metrics of enhanced
319 IVT (depending on the metric used). To determine if these numbers of events are statistically significant, we
320 performed a bootstrap on the calving events in our catalog (see also the description in the Methods). When
321 our bootstrap is applied to all calving events in our catalog, we find no statistically significant relationship
322 for the 28-day metrics of IVT (Table 1). However, we do find a statistically significant relationship for the
323 7-day metrics of IVT, with a probability of spurious correlation less than 2%. Hence, even though only 9
324 of the 41 events were associated with enhanced 7-day averaged metrics of IVT, this amount of events is
325 unlikely to be caused by random chance and the correlation is statistically significant. This relationship is
326 broadly consistent with Wille and others (2022), but applies to a wider set of ice shelves that span most
327 of the Antarctic ice sheet.

328 **Regional sensitivity to enhanced IVT**

329 To determine if there are regional differences in the relationship between the metrics of IVT and iceberg
330 calving, we separately applied our bootstrap to the calving events in the Antarctic Peninsula and the
331 Amundsen Sea Embayment. These two regions experience contrasting meteorological and glaciological
332 environments, and are the only regions that have enough events in our catalog to perform statistical
333 tests. Our bootstrap shows that none of our metrics of IVT have a statistically significant relationship
334 with calving events from the Amundsen Sea Embayment (Table 1). However, we do find a statistically
335 significant relationship for the Antarctic Peninsula that mirrors that of our Antarctic-wide bootstrap: the
336 28-day metrics of IVT show no statistical significance, but we do see a statistically significant relationship
337 between calving and both 7-day metrics of IVT.

338 **Sensitivity to IVT threshold**

339 It is possible that our results are sensitive to our chosen 90th percentile threshold that defines when metrics
340 of IVT are considered “enhanced.” To test this, we performed additional tests where we varied the threshold
341 from the 80th to 95th percentile (see Table 2). The sensitivity test bolsters our previous results: we find
342 that for the ice sheet-wide and the Antarctic Peninsula bootstrap both of our metrics of 7-day IVT remain
343 statistically significant for thresholds that range from the 80th-90th percentiles. For the Amundsen Sea

Table 1. The number of calving events in the catalog that have enhanced IVT^T and IVT^V , both for Antarctic-wide events, and those from the respective Amundsen Sea Embayment and the Antarctic Peninsula regions. The probability of spurious correlation between real events and enhanced metrics of IVT is given in parentheses beside each count. Reported probabilities are rounded to the nearest integer percentage. Percent values below 5% (i.e. those considered significant at the 95% level) are bolded.

	Antarctic-wide (41 events)		Amundsen Sea Embayment (13 events)		Antarctic Peninsula (8 events)	
	28 day	7 day	28 day	7 day	28 day	7 day
IVT^T	6 (30%)	9 (2%)	3 (14%)	3 (14%)	2 (23%)	3 (4%)
IVT^V	6 (25%)	9 (2%)	2 (29%)	3 (13%)	3 (8%)	3 (4%)

344 Embayment, there is no consistent pattern of statistical significance for any threshold that we examined,
 345 although there are isolated metrics and thresholds that show significance. For example, IVT_{28}^T is the only
 346 metric statistically significant at the 85th percentile threshold, but IVT_{28}^T is not statistically significant for
 347 any other threshold we examined. Similarly, IVT_{28}^V for the Amundsen Sea Embayment was significant for
 348 the 95th percentile, but no other threshold. This suggests that our metrics of IVT show sensitivity to the
 349 choice of percentile threshold.

350 DISCUSSION

351 Most calving events are not triggered by atmospheric moisture transport

352 Contrary to recent studies that suggest that extreme moisture transport acts as a trigger for calving (Wille
 353 and others, 2022; Francis and others, 2021, 2022; Wille and others, 2024), most of the calving events in our
 354 catalog are not associated with enhanced metrics of IVT (defined as the 90th percentile). This suggests
 355 that, at the very least, enhanced moisture transport is not a *necessary* condition to trigger tabular iceberg
 356 calving. Nonetheless, we do see a statistically significant fraction of calving events that are correlated with
 357 the 7-day metrics of IVT.

358 We also see regional differences in the statistical significance of the correlation between enhanced met-
 359 rics of IVT and the timing of iceberg calving. For instance, the Antarctic Peninsula appears to show a
 360 relationship with statistical significance for both of the 7-day metrics of IVT, a result that holds whether
 361 we set the threshold for enhancement at the 85th or 90th percentiles. This result is consistent with previous
 362 studies that show how extreme moisture transport over the Antarctic Peninsula was coincident with the

Table 2. The number of calving events that have IVT^T and IVT^V that exceeds the 80th, 85th, 90th, and 95th percentiles for those in the Amundsen Sea Embayment and the Antarctic Peninsula. The probability of spurious correlation between real events and enhanced metrics of IVT (as defined at each percentile threshold) is given in parentheses beside each count. Reported probabilities are rounded to the nearest integer percentage. Percent values below 5% (i.e. those considered significant at the 95% level) are bolded.

	80th		85th		90th		95th	
	28 day	7 day	28 day	7 day	28 day	7 day	28 day	7 day
Amundsen Sea Embayment								
IVT^T	6 (3%)	3 (50%)	4 (14%)	3 (31%)	3 (14%)	3 (14%)	2 (8%)	2 (13%)
IVT^V	5 (8%)	4 (25%)	5 (2%)	3 (32%)	2 (28%)	3 (13%)	2 (8%)	3 (2%)
Antarctic Peninsula								
IVT^T	3 (20%)	5 (1%)	3 (12%)	5 (0%)	2 (23%)	3 (4%)	2 (8%)	1 (33%)
IVT^V	6 (0%)	4 (6%)	3 (14%)	4 (2%)	3 (8%)	3 (4%)	1 (50%)	2 (6%)

363 rapid disintegration of the Larsen A and B Ice Shelves (Wille and others, 2022; Laffin and others, 2022).
 364 This pattern of statistical significance contrasts with our findings for the Amundsen Sea Embayment ice
 365 shelves, which do not appear to exhibit any consistent pattern showing a statistically significant correlation
 366 for any metrics of enhanced IVT. The discrepancy between these two regions is broadly consistent with
 367 ocean-driven retreat in the Amundsen Sea Embayment (Kimura and others, 2017; Nakayama and others,
 368 2019).

369 It is possible that the regional differences between the Amundsen Sea Embayment and Antarctic Penin-
 370 sula ice shelves extend to other ice shelves. However, the scarcity of calving events from the other ice shelves
 371 examined precludes a meaningful statistical analysis for most other regions unless we entertain geograph-
 372 ically broad groupings, like all ice shelves that fringe the East Antarctic Ice Sheet. Given the difference
 373 between the Amundsen Sea Embayment and Antarctic Peninsula, however, it seems likely that conditional
 374 factors that differ between regions—and perhaps individual ice shelves—that may result in greater sensi-
 375 tivity of tabular calving to enhanced IVT in some circumstances. Extending the time frame of our analysis
 376 to earlier than our 2013 start date could reveal additional regions that may be sensitive to enhanced IVT.
 377 On the other hand, because we compute monthly percentiles of the metrics of IVT from 1979–2023, trends
 378 in IVT over Antarctic ice shelves due to climate change may cause our study to overstate the statistical

379 significance of the association of enhanced metrics of IVT with iceberg calving (Payne and others, 2020;
380 Maclennan and others, 2023).

381 **Attribution of calving triggers from case studies can be misleading**

382 Our results also emphasize that caution is needed when evaluating statistical significance without physical
383 mechanisms to link calving to specific choices of both metrics of IVT and thresholds on it. Previous studies
384 linked calving events from the Amery, Brunt, and Conger ice shelves to elevated conditions of anomalous
385 atmospheric moisture transport (Francis and others, 2021, 2022; Wille and others, 2024). However, in
386 our work, each of the calving events from those ice shelves corresponded to 7- and 28-day metrics of IVT
387 that ranged from the 80th to the 89th percentiles, and were therefore not associated with enhanced IVT.
388 This indicates that the moisture transport conditions over the ice shelves prior to their calving events
389 examined by the case studies detailed in Francis and others (2021, 2022); Wille and others (2024) are high
390 (above the 80th percentile), but not particularly rare occurrences. Wille and others (2022) identified an
391 atmospheric river prior to the July 2017 calving event from the Larsen C ice shelf, which in our study
392 corresponded to enhanced IVT_{28}^V and IVT_7^V . Our results suggest that the connection between iceberg
393 calving and atmospheric rivers found for the Antarctic Peninsula by Wille and others (2022) is limited
394 to that region. Moreover, we found some metrics of IVT that resulted in isolated calving events being
395 identified as coincident with “enhanced” metrics of IVT, but no statistically significant relationship when
396 applied to a larger set of calving events. Finally, because tabular calving typically has a much longer
397 recurrence interval than enhanced IVT at the thresholds we examined, most incidences of enhanced IVT
398 over the ice shelves we examined are not coincident with calving. This suggests that correlation between
399 calving and IVT we observed may have little predictive power. For instance, as we decrease the percentile
400 threshold, we also observe a much larger number of enhanced IVT events that are not associated with
401 any calving event. For example, the Ronne Ice Shelf saw at least 80th percentile IVT_7^T 92 times from
402 2013–23, compared to 49 instances of 90th percentile IVT_7^T over the same ice shelf. This is still much more
403 frequent than the number of calving events from the Ronne Ice Shelf, which occurred only once in the
404 study period. Therefore, while enhanced IVT may be significantly correlated with the timing of calving
405 for a minority of the calving events, it still may have low predictive power in determining when iceberg
406 calving events occur. This is consistent with the fact that, at least at the 90th percentile, ~80% of calving
407 events are not associated with any enhanced metrics of IVT. As we decrease the threshold, the number of

408 events associated with metrics of IVT increase, but so do the number of instances when IVT exceeds the
409 threshold without a simultaneous calving event.

410 It is also possible that, although enhanced IVT itself has little predictive power, the correlation with
411 calving is statistically significant because IVT covaries with other environmental variables that may have
412 a more direct mechanical connection to the calving process. For instance, enhanced IVT is connected with
413 warm air advection and consequently anomalously high temperatures, which can result in surface melt
414 (Bozkurt and others, 2018; Wille and others, 2019; Djoumna and Holland, 2021; Adusumilli and others,
415 2021; Gorodetskaya and others, 2023). Enhanced IVT is also associated with conditions that result in
416 higher wind speeds, sea surface slopes, and sea ice clearing, which have also been hypothesized to impact
417 iceberg calving Arthur and others (2021); Francis and others (2021, 2022); Wille and others (2024). Our
418 study can only determine if the observed correlation between enhanced metrics of IVT and calving is
419 statistically significant and does not inform us about the potential causal mechanisms that link enhanced
420 IVT to calving.

421 **Our methodology can be extended to other environmental triggers**

422 The methodology we applied here can be applied to a variety of potential triggers. For example, Table
423 3 shows the results of our bootstrap applied to the 10 m wind speed and 2 m atmospheric temperature
424 using a 90th percentile threshold. We see no statistically significant correlation between calving and wind
425 speed. However, we do see a statistically significant correlation with 2 m temperature. Here we see that all
426 calving events that have enhanced IVT also have enhanced 2 m temperature. At first glance, the connection
427 between calving and atmospheric temperature is not surprising given the link between surface melt and
428 hydrofracture (Scambos and others, 2000; van den Broeke, 2005; Robel and Banwell, 2019). However, the
429 correlation we see is apparent through analysis of synoptic- to up to weekly-scale variations of temperature.
430 This diverges from current theory which suggests sensitivity of ice shelves to surface melt and hydrofracture
431 requires longer-term depletion of firn-air content (Kuipers Munneke and others, 2014; Machguth and others,
432 2016; Robel and Banwell, 2019). Given the potential for biases in ERA 2 m temperatures, and the fact
433 that the correlation between calving and temperature may also not be causal, we view this connection
434 between 2 m temperature and calving as it appears here as speculative. Nonetheless, it illustrates that we
435 can begin to perform more systematic attribution studies given a large enough catalog of icebergs.

Table 3. The number of calving events that have enhanced 2 m temperature and 10 m wind speed for each in the catalog, both Antarctic-wide, and for the events from ice shelves surrounding the Amundsen Sea Embayment, and the Antarctic Peninsula. The probabilities of spurious correlations between real events and enhanced 2 m temperature and 10 m wind speed are given in parentheses beside each count. Reported probabilities are rounded to the nearest integer percentage. Percent values below 5% (i.e. those considered significant at the 95% level) are bolded.

	Antarctic-wide (41 events)		Amundsen Sea Embayment (13 events)		Antarctic Peninsula (8 events)	
	28 day	7 day	28 day	7 day	28 day	7 day
2 m temperature	15 (0%)	11 (0%)	7 (0%)	4 (4%)	2 (47%)	3 (5%)
10 m wind speed	7 (11%)	3 (79%)	1 (69%)	1 (73%)	1 (68%)	1 (69%)

436 **CONCLUSIONS**

437 We investigated the extent by which enhanced atmospheric water vapor transport over Antarctic ice shelves
438 is correlated with tabular iceberg calving events by examining metrics of IVT derived from ERA5 reanalysis.
439 We found that a majority of calving events (approximately 80%) are not associated with any of our metrics
440 of enhanced IVT. However, the fraction of tabular iceberg calving events that had enhanced metrics of
441 7-day IVT occurred at a greater frequency than would be expected solely from the climatology if no
442 relationship existed. This correlation was statistically significant when applied either continent-wide or to
443 the Antarctic Peninsula specifically. The relationship was insensitive to specific definitions of the 7-day
444 metric or threshold used to define “enhanced”. By contrast, we saw no statistically significant correlation
445 between metrics of enhanced IVT and ice shelves in the Amundsen Sea Embayment, suggesting that triggers
446 for iceberg calving are, not surprisingly, regionally-specific.

447 Antarctic ice shelves are expected to become more vulnerable to atmospheric air temperature extremes
448 through the 21st century, particularly in ice shelves in typically dry regions (Gilbert and Kittel, 2021; van
449 Wessem and others, 2023). Furthermore, atmospheric rivers in the future are expected to become more
450 frequent and intense (Payne and others, 2020; Maclennan and others, 2023). Therefore, it is likely that
451 we will see more icebergs that detach during periods when enhanced atmospheric moisture transport is
452 occurring. However, because calving events occur much less frequently than any of our enhanced metrics of
453 IVT, it seems unlikely IVT is the primary driver of calving events. Instead, it seems more likely that when
454 ice shelves evolve into a state where rifts nearly isolate an iceberg, the timing of the final calving event
455 shows increased sensitivity to modest levels of IVT. This would imply that, although the mechanical impact
456 of enhanced IVT, sea slope, winds and other variables is small most of the time (e.g., Bassis and others,
457 2008), as ice shelves become more fractured and rifts come closer to isolating icebergs, these variables
458 become more important. If this is the case, then as ice shelves continue to evolve under future climate
459 warming, we are likely to see more ice shelves preconditioned to be more sensitive to enhanced IVT or
460 other environmental forcing. However, it is the processes governing preconditioning that will control the
461 future stability of ice shelves.

462 Tabular iceberg calving is a sporadic process on Antarctic ice shelves that can have minimal impact on
463 the mass balance of the Antarctic Ice Sheet at the present (Fricker and others, 2002; Bassis and others,
464 2024). However, if the mass removed by the calving event reduces the buttressing force on the Antarctic

465 Ice Sheet due to the ice shelf, accelerated mass flux across the grounding line of the ice sheet can increase
466 discharge into the oceans (Dupont and Alley, 2005; Gudmundsson and others, 2019; Marsh and others,
467 2024). The increased mass flux into the ocean can raise the net contribution of the Antarctic Ice Sheet
468 to the rate of sea level rise. However, increased atmospheric water vapor transport and more frequent
469 atmospheric river landfalls across the ice sheet can increase the amount of snowfall, effectively offsetting
470 mass losses through the ice shelves (Wille and others, 2021; MacLennan and others, 2023; Davison, 2023;
471 Park and others, 2023; Rendfrey and others, 2024). Furthermore, although we have found that connection
472 between enhanced IVT and calving is, at best, weak, it is possible that there is a stronger connection with
473 ice shelf rift propagation that precedes calving. Alternative methods to describe change on the ice sheet, for
474 example, the detection of crevasses and their evolution described in Li and others (2024) could be applied
475 in conjunction with analysis of enhanced atmospheric water vapor transport in future work. However,
476 our study remains limited to assessing correlation and still cannot determine causality, which requires a
477 physical mechanism linking atmospheric extremes to calving or rift propagation. The diverging potential
478 consequences of enhanced atmospheric moisture transport on Antarctic surface processes therefore remains
479 a large source of uncertainty in projections of Antarctic Ice Sheet mass balance and, consequently, future
480 rates of sea level rise. Further investigation of the physical processes linking enhanced atmospheric moisture
481 transport to surface conditions on Antarctic ice shelves may contribute to reducing such uncertainty.

482 **ACKNOWLEDGEMENTS**

483 This work is funded by DoE grant C3710, Framework for Antarctic System Science in E3SM, NASA
484 grant 80NSSC22K0378 and by the DOMINOS project, a component of the International Thwaites Glacier
485 Collaboration (ITGC), with support from National Science Foundation (NSF: Grant 1738896) and Natural
486 Environment Research Council (NERC: Grant NE/S006605/1). ITGC Contribution No. ITGC-XXX.

487 **REFERENCES**

- 488 Adusumilli S, Fish M, Fricker HA and Medley B (2021) Atmospheric river precipitation contributed to rapid increases
489 in surface height of the West Antarctic Ice Sheet in 2019. *Geophysical Research Letters*, **48**(5), ISSN 0094-8276,
490 1944-8007 (doi: 10.1029/2020GL091076)
- 491 Alley R, Cuffey K, Bassis J, Alley K, Wang S, Parizek B, Anandakrishnan S, Christianson K and DeConto R (2023)
492 Iceberg calving: Regimes and transitions. *Annual Review of Earth and Planetary Sciences*, **51**(1), 189–215, ISSN
493 1545-4495 (doi: 10.1146/annurev-earth-032320-110916)
- 494 Amundson JM and Truffer M (2010) A unifying framework for iceberg-calving models. *Journal of Glaciology*, **56**(199),
495 822–830, ISSN 1727-5652 (doi: 10.3189/002214310794457173)
- 496 Arthur JF, Stokes CR, Jamieson SSR, Miles BWJ, Carr JR and Leeson AA (2021) The triggers of the disaggregation
497 of Voyeykov Ice Shelf (2007), Wilkes Land, East Antarctica, and its subsequent evolution. *Journal of Glaciology*,
498 **67**(265), 933–951, ISSN 1727-5652 (doi: 10.1017/jog.2021.45)
- 499 Banwell AF, MacAyeal DR and Sergienko OV (2013) Breakup of the Larsen B Ice Shelf triggered by chain re-
500 action drainage of supraglacial lakes. *Geophysical Research Letters*, **40**(22), 5872–5876, ISSN 0094-8276 (doi:
501 10.1002/2013gl057694)
- 502 Bassis JN and Jacobs S (2013) Diverse calving patterns linked to glacier geometry. *Nature Geoscience*, **6**(10), 833–836,
503 ISSN 1752-0908 (doi: 10.1038/ngeo1887), publisher: Nature Publishing Group
- 504 Bassis JN and Walker CC (2011) Upper and lower limits on the stability of calving glaciers from the yield strength
505 envelope of ice. *Proceedings of the Royal Society A: Mathematical, Physical and Engineering Sciences*, **468**(2140),
506 913–931, ISSN 1471-2946 (doi: 10.1098/rspa.2011.0422)
- 507 Bassis JN, Fricker HA, Coleman R and Minster JB (2008) An investigation into the forces that drive ice-shelf rift
508 propagation on the Amery Ice Shelf, East Antarctica. *Journal of Glaciology*, **54**(184), 17–27, ISSN 1727-5652 (doi:
509 10.3189/002214308784409116)
- 510 Bassis JN, Crawford A, Kachuck SB, Benn DI, Walker C, Millstein J, Duddu R, Åström J, Fricker H and Luckman A
511 (2024) Stability of ice shelves and ice cliffs in a changing climate. *Annual Review of Earth and Planetary Sciences*,
512 **52**(1), ISSN 1545-4495 (doi: 10.1146/annurev-earth-040522-122817)
- 513 Benn DI, Luckman A, Åström JA, Crawford AJ, Cornford SL, Bevan SL, Zwinger T, Gladstone R, Alley K, Pettit E
514 and Bassis J (2022) Rapid fragmentation of Thwaites Eastern Ice Shelf. *The Cryosphere*, **16**(6), 2545–2564, ISSN
515 1994-0424 (doi: 10.5194/tc-16-2545-2022)

- 516 Bozkurt D, Rondanelli R, Marín JC and Garreaud R (2018) Foehn event triggered by an atmospheric river underlies
517 record-setting temperature along continental Antarctica. *Journal of Geophysical Research: Atmospheres*, **123**(8),
518 3871–3892, ISSN 2169897X (doi: 10.1002/2017JD027796)
- 519 Bozkurt D, Marín JC and Barrett BS (2022) Temperature and moisture transport during atmospheric block-
520 ing patterns around the Antarctic Peninsula. *Weather and Climate Extremes*, 100506, ISSN 22120947 (doi:
521 10.1016/j.wace.2022.100506)
- 522 Bromirski PD, Sergienko OV and MacAyeal DR (2010) Transoceanic infragravity waves impacting Antarctic ice
523 shelves. *Geophysical Research Letters*, **37**(2), ISSN 1944-8007 (doi: 10.1029/2009GL041488)
- 524 Budge JS and Long DG (2018) A comprehensive database for Antarctic iceberg tracking using scatterometer data.
525 *IEEE Journal of Selected Topics in Applied Earth Observations and Remote Sensing*, **11**(2), 434–442, ISSN 2151-
526 1535 (doi: 10.1109/jstars.2017.2784186)
- 527 Camuffo D, Becherini F and della Valle A (2020) Relationship between selected percentiles and return periods of
528 extreme events. *Acta Geophysica*, **68**(4), 1201–1211, ISSN 1895-7455 (doi: 10.1007/s11600-020-00452-x)
- 529 Clem KR, Bozkurt D, Kennett D, King JC and Turner J (2022) Central tropical pacific convection drives extreme
530 high temperatures and surface melt on the Larsen C Ice Shelf, Antarctic Peninsula. *Nature Communications*,
531 **13**(1), ISSN 2041-1723 (doi: 10.1038/s41467-022-31119-4)
- 532 Costi J, Arigony-Neto J, Braun M, Mavlyudov B, Barrand NE, da Silva AB, Marques WC and Simões JC (2018)
533 Estimating surface melt and runoff on the Antarctic Peninsula using ERA-Interim reanalysis data. *Antarctic*
534 *Science*, **30**(6), 379–393, ISSN 1365-2079 (doi: 10.1017/s0954102018000391)
- 535 Crosson WL, Al-Hamdan MZ, Hemmings SNJ and Wade GM (2012) A daily merged MODIS Aqua–Terra land
536 surface temperature data set for the conterminous United States. *Remote Sensing of Environment*, **119**, 315–324,
537 ISSN 0034-4257 (doi: 10.1016/j.rse.2011.12.019)
- 538 Davison BJ (2023) Sea level rise from West Antarctic mass loss significantly modified by large snowfall anomalies.
539 *Nature Communications*
- 540 Davison BJ, Hogg AE, Gourmelen N, Jakob L, Wuite J, Nagler T, Greene CA, Andreasen J and Engdahl ME (2023)
541 Annual mass budget of Antarctic ice shelves from 1997 to 2021. *Science Advances*, **9**(41), ISSN 2375-2548 (doi:
542 10.1126/sciadv.adi0186)
- 543 DeConto RM and Pollard D (2016) Contribution of Antarctica to past and future sea-level rise. *Nature*, **531**(7596),
544 591–597, ISSN 1476-4687 (doi: 10.1038/nature17145)

- 545 Depoorter MA, Bamber JL, Griggs JA, Lenaerts JTM, Ligtenberg SRM, van den Broeke MR and Moholdt G (2013)
546 Calving fluxes and basal melt rates of Antarctic ice shelves. *Nature*, **502**(7469), 89–92, ISSN 1476-4687 (doi:
547 10.1038/nature12567)
- 548 Djoumna G and Holland DM (2021) Atmospheric rivers, warm air intrusions, and surface radiation balance in the
549 Amundsen Sea Embayment. *Journal of Geophysical Research: Atmospheres*, **126**(13), ISSN 2169-897X, 2169-8996
550 (doi: 10.1029/2020JD034119)
- 551 Dupont TK and Alley RB (2005) Assessment of the importance of ice-shelf buttressing to ice-sheet flow. *Geophysical*
552 *Research Letters*, **32**(4), ISSN 1944-8007 (doi: 10.1029/2004gl022024)
- 553 Dziak RP, Lee WS, Haxel JH, Matsumoto H, Tepp G, Lau TK, Roche L, Yun S, Lee CK, Lee J and Yoon ST (2019)
554 Hydroacoustic, meteorologic and seismic observations of the 2016 Nansen Ice Shelf calving event and iceberg
555 formation. *Frontiers in Earth Science*, **7**, ISSN 2296-6463 (doi: 10.3389/feart.2019.00183)
- 556 Edwards TL, Brandon MA, Durand G, Edwards NR, Golledge NR, Holden PB, Nias IJ, Payne AJ, Ritz C and
557 Wernecke A (2019) Revisiting Antarctic ice loss due to marine ice-cliff instability. *Nature*, **566**(7742), 58–64, ISSN
558 1476-4687 (doi: 10.1038/s41586-019-0901-4)
- 559 Efron B (1979) Computers and the theory of statistics: Thinking the unthinkable. *SIAM Review*, **21**(4), 460–480,
560 ISSN 1095-7200 (doi: 10.1137/1021092)
- 561 England MR, Wagner TJW and Eisenman I (2020) Modeling the breakup of tabular icebergs. *Science Advances*,
562 **6**(51), ISSN 2375-2548 (doi: 10.1126/sciadv.abd1273)
- 563 Espinoza V, Waliser DE, Guan B, Lavers DA and Ralph FM (2018) Global analysis of climate change pro-
564 jection effects on atmospheric rivers. *Geophysical Research Letters*, **45**(9), 4299–4308, ISSN 1944-8007 (doi:
565 10.1029/2017gl076968)
- 566 Francis D, Mattingly KS, Lhermitte S, Temimi M and Heil P (2021) Atmospheric extremes caused high oceanward
567 sea surface slope triggering the biggest calving event in more than 50 years at the Amery ice shelf. *The Cryosphere*,
568 **15**(5), 2147–2165, ISSN 1994-0424 (doi: 10.5194/tc-15-2147-2021)
- 569 Francis D, Fonseca R, Mattingly KS, Marsh OJ, Lhermitte S and Cherif C (2022) Atmospheric triggers of the Brunt
570 ice shelf calving in February 2021. *Journal of Geophysical Research: Atmospheres*, **127**(11), ISSN 2169-8996 (doi:
571 10.1029/2021jd036424)
- 572 Fricker HA, Young NW, Allison I and Coleman R (2002) Iceberg calving from the Amery ice shelf, East Antarctica.
573 *Annals of Glaciology*, **34**, 241–246, ISSN 1727-5644 (doi: 10.3189/172756402781817581)

- 574 Gagliardini O, Durand G, Zwinger T, Hindmarsh RCA and Le Meur E (2010) Coupling of ice-shelf melting and
575 buttressing is a key process in ice-sheets dynamics. *Geophysical Research Letters*, **37**(14), ISSN 1944-8007 (doi:
576 10.1029/2010gl043334)
- 577 Garbe J, Albrecht T, Levermann A, Donges JF and Winkelmann R (2020) The hysteresis of the Antarctic Ice Sheet.
578 *Nature*, **585**(7826), 538–544, ISSN 1476-4687 (doi: 10.1038/s41586-020-2727-5)
- 579 Gilbert E and Kittel C (2021) Surface melt and runoff on Antarctic ice shelves at 1.5°C, 2°C, and 4°C of future
580 warming. *Geophysical Research Letters*, **48**(8), ISSN 1944-8007 (doi: 10.1029/2020gl091733)
- 581 Gimeno L, Nieto R, Vazquez M and Lavers DA (2014) Atmospheric rivers: a mini-review. *Frontiers in Earth Science*,
582 **2**, ISSN 2296-6463 (doi: 10.3389/feart.2014.00002)
- 583 Glasser N and Scambos T (2008) A structural glaciological analysis of the 2002 Larsen B ice-shelf collapse. *Journal*
584 *of Glaciology*, **54**(184), 3–16, ISSN 1727-5652 (doi: 10.3189/002214308784409017)
- 585 Goldberg D, Holland DM and Schoof C (2009) Grounding line movement and ice shelf buttressing in marine ice
586 sheets. *Journal of Geophysical Research: Earth Surface*, **114**(F4), ISSN 0148-0227 (doi: 10.1029/2008jf001227)
- 587 Gorodetskaya IV, Tsukernik M, Claes K, Ralph MF, Neff WD and Van Lipzig NPM (2014) The role of atmospheric
588 rivers in anomalous snow accumulation in East Antarctica. *Geophysical Research Letters*, **41**(17), 6199–6206, ISSN
589 00948276 (doi: 10.1002/2014GL060881)
- 590 Gorodetskaya IV, Durán-Alarcón C, González-Herrero S, Clem KR, Zou X, Rowe P, Rodriguez Imazio P, Campos
591 D, Leroy-Dos Santos C, Dutrievoz N, Wille JD, Chyhareva A, Favier V, Blanchet J, Pohl B, Cordero RR, Park
592 SJ, Colwell S, Lazzara MA, Carrasco J, Gulisano AM, Krakovska S, Ralph FM, Dethinne T and Picard G (2023)
593 Record-high Antarctic Peninsula temperatures and surface melt in February 2022: a compound event with an
594 intense atmospheric river. *npj Climate and Atmospheric Science*, **6**(1), ISSN 2397-3722 (doi: 10.1038/s41612-023-
595 00529-6)
- 596 Greene CA, Gardner AS, Schlegel NJ and Fraser AD (2022) Antarctic calving loss rivals ice-shelf thinning. *Nature*,
597 **609**(7929), 948–953, ISSN 1476-4687 (doi: 10.1038/s41586-022-05037-w)
- 598 Gudmundsson GH (2013) Ice-shelf buttressing and the stability of marine ice sheets. *The Cryosphere*, **7**(2), 647–655,
599 ISSN 1994-0424 (doi: 10.5194/tc-7-647-2013)
- 600 Gudmundsson GH, Paolo FS, Adusumilli S and Fricker HA (2019) Instantaneous Antarctic Ice Sheet mass loss
601 driven by thinning ice shelves. *Geophysical Research Letters*, **46**(23), 13903–13909, ISSN 0094-8276, 1944-8007
602 (doi: 10.1029/2019GL085027)

- 603 Hersbach H, Bell B, Berrisford P, Hirahara S, Horányi A, Muñoz-Sabater J, Nicolas J, Peubey C, Radu R, Schepers
604 D, Simmons A, Soci C, Abdalla S, Abellan X, Balsamo G, Bechtold P, Biavati G, Bidlot J, Bonavita M, Chiara
605 G, Dahlgren P, Dee D, Diamantakis M, Dragani R, Flemming J, Forbes R, Fuentes M, Geer A, Haimberger L,
606 Healy S, Hogan RJ, Hólm E, Janisková M, Keeley S, Laloyaux P, Lopez P, Lupu C, Radnoti G, Rosnay P, Rozum
607 I, Vamborg F, Villaume S and Thépaut J (2020) The ERA5 global reanalysis. *Quarterly Journal of the Royal
608 Meteorological Society*, **146**(730), 1999–2049, ISSN 0035-9009, 1477-870X (doi: 10.1002/qj.3803)
- 609 Humbert A and Steinhage D (2011) The evolution of the western rift area of the Fimbul Ice Shelf, Antarctica. *The
610 Cryosphere*, **5**(4), 931–944, ISSN 1994-0416 (doi: 10.5194/tc-5-931-2011)
- 611 Indrigo C, Dow CF, Greenbaum JS and Morlighem M (2020) Drygalski ice tongue stability influenced by rift formation
612 and ice morphology. *Journal of Glaciology*, **67**(262), 243–252, ISSN 1727-5652 (doi: 10.1017/jog.2020.99)
- 613 Joughin I and MacAyeal DR (2005) Calving of large tabular icebergs from ice shelf rift systems. *Geophysical Research
614 Letters*, **32**(2), ISSN 1944-8007 (doi: 10.1029/2004gl020978)
- 615 Kenneally J and Hughes T (2006) Calving giant icebergs: old principles, new applications. *Antarctic Science*, **18**(3),
616 409–419, ISSN 1365-2079 (doi: 10.1017/s0954102006000459)
- 617 Kimura S, Jenkins A, Regan H, Holland PR, Assmann KM, Whitt DB, Van Wessem M, van de Berg WJ, Reijmer
618 CH and Dutrieux P (2017) Oceanographic controls on the variability of ice-shelf basal melting and circulation
619 of glacial meltwater in the Amundsen Sea Embayment, Antarctica. *Journal of Geophysical Research: Oceans*,
620 **122**(12), 10131–10155, ISSN 2169-9291 (doi: 10.1002/2017jc012926)
- 621 Kuipers Munneke P, Picard G, van den Broeke MR, Lenaerts JTM and van Meijgaard E (2012) Insignificant
622 change in Antarctic snowmelt volume since 1979. *Geophysical Research Letters*, **39**(1), ISSN 1944-8007 (doi:
623 10.1029/2011gl050207)
- 624 Kuipers Munneke P, Ligtenberg SR, van den Broeke MR and Vaughan DG (2014) Firn air depletion as a precursor of
625 Antarctic ice-shelf collapse. *Journal of Glaciology*, **60**(220), 205–214, ISSN 1727-5652 (doi: 10.3189/2014jog13j183)
- 626 Kuipers Munneke P, Luckman AJ, Bevan SL, Smeets CJPP, Gilbert E, van den Broeke MR, Wang W, Zender C,
627 Hubbard B, Ashmore D, Orr A, King JC and Kulesa B (2018) Intense winter surface melt on an Antarctic ice
628 shelf. *Geophysical Research Letters*, **45**(15), 7615–7623, ISSN 1944-8007 (doi: 10.1029/2018gl077899)
- 629 Laffin MK, Zender CS, van Wessem M and Marinsek S (2022) The role of föhn winds in eastern Antarctic peninsula
630 rapid ice shelf collapse. *The Cryosphere*, **16**(4), 1369–1381, ISSN 1994-0424 (doi: 10.5194/tc-16-1369-2022)
- 631 Lazzara MA, Jezek KC, Scambos TA, MacAyeal DR and van der Veen CJ (1999) On the recent calving of icebergs
632 from the Ross Ice Shelf. *Polar Geography*, **23**(3), 201–212, ISSN 1939-0513 (doi: 10.1080/10889379909377676)

- 633 Legrésy B, Wendt A, Tabacco I, Rémy F and Dietrich R (2004) Influence of tides and tidal current
634 on Mertz Glacier, Antarctica. *Journal of Glaciology*, **50**(170), 427–435, ISSN 0022-1430, 1727-5652 (doi:
635 10.3189/172756504781829828)
- 636 Lenaerts JTM, Medley B, van den Broeke MR and Wouters B (2019) Observing and modeling ice sheet surface mass
637 balance. *Reviews of Geophysics*, **57**(2), 376–420, ISSN 1944-9208 (doi: 10.1029/2018rg000622)
- 638 Lescarmonnier L, Legresy B, Young NW, Coleman R, Testut L, Mayet C and Lacroix P (2015) Rifting processes and
639 ice-flow modulation observed on Mertz Glacier, East Antarctica. *Journal of Glaciology*, **61**(230), 1183–1193, ISSN
640 0022-1430, 1727-5652 (doi: 10.3189/2015JoG15J028)
- 641 Li Q, An J, Xing Z, Wang Z, Jiang P, Yan B, Wu Y and Zhang B (2024) Three-dimensional dynamic monitoring of
642 crevasses based on deep learning and surface elevation reconstruction methods. *International Journal of Applied
643 Earth Observation and Geoinformation*, **132**, 104017, ISSN 1569-8432 (doi: 10.1016/j.jag.2024.104017)
- 644 Lipovsky BP (2020) Ice shelf rift propagation: stability, three-dimensional effects, and the role of marginal weakening.
645 *The Cryosphere*, **14**(5), 1673–1683, ISSN 1994-0424 (doi: 10.5194/tc-14-1673-2020)
- 646 Liu Y, Moore JC, Cheng X, Gladstone RM, Bassis JN, Liu H, Wen J and Hui F (2015) Ocean-driven thinning
647 enhances iceberg calving and retreat of Antarctic ice shelves. *Proceedings of the National Academy of Sciences*,
648 **112**(11), 3263–3268, ISSN 1091-6490 (doi: 10.1073/pnas.1415137112)
- 649 MacAyeal DR, Okal EA, Aster RC, Bassis JN, Brunt KM, Cathles LM, Drucker R, Fricker HA, Kim YJ, Martin S,
650 Okal MH, Sergienko OV, Sponsler MP and Thom JE (2006) Transoceanic wave propagation links iceberg calving
651 margins of Antarctica with storms in tropics and Northern Hemisphere. *Geophysical Research Letters*, **33**(17),
652 ISSN 1944-8007 (doi: 10.1029/2006GL027235)
- 653 Machguth H, MacFerrin M, van As D, Box JE, Charalampidis C, Colgan W, Fausto RS, Meijer HAJ, Mosley-
654 Thompson E and van de Wal RSW (2016) Greenland meltwater storage in firn limited by near-surface ice formation.
655 *Nature Climate Change*, **6**(4), 390–393, ISSN 1758-6798 (doi: 10.1038/nclimate2899)
- 656 MacLennan ML, Lenaerts JTM, Shields CA, Hoffman AO, Wever N, Thompson-Munson M, Winters AC, Pettit EC,
657 Scambos TA and Wille JD (2023) Climatology and surface impacts of atmospheric rivers on West Antarctica. *The
658 Cryosphere*, **17**(2), 865–881, ISSN 1994-0424 (doi: 10.5194/tc-17-865-2023)
- 659 Marsh OJ, Luckman AJ and Hodgson DA (2024) Brief communication: Rapid acceleration of the Brunt Ice Shelf
660 after calving of iceberg A-81. *The Cryosphere*, **18**(2), 705–710, ISSN 1994-0424 (doi: 10.5194/tc-18-705-2024)
- 661 Massom RA, Scambos TA, Bennetts LG, Reid P, Squire VA and Stammerjohn SE (2018) Antarctic ice shelf disintegra-
662 tion triggered by sea ice loss and ocean swell. *Nature*, **558**(7710), 383–389, ISSN 1476-4687 (doi: 10.1038/s41586-
663 018-0212-1)

- 664 Mayet C, Testut L, Legresy B, Lescarmonier L and Lyard F (2013) High-resolution barotropic modeling and the
665 calving of the Mertz Glacier, East Antarctica. *Journal of Geophysical Research: Oceans*, **118**(10), 5267–5279, ISSN
666 2169-9275 (doi: 10.1002/jgrc.20339)
- 667 Miles BWJ, Stokes CR, Jamieson SSR, Jordan JR, Gudmundsson GH and Jenkins A (2022) High spatial and temporal
668 variability in Antarctic ice discharge linked to ice shelf buttressing and bed geometry. *Scientific Reports*, **12**(1),
669 ISSN 2045-2322 (doi: 10.1038/s41598-022-13517-2)
- 670 Mouginot J (2017) Measures Antarctic boundaries for ipy 2007-2009 from satellite radar, version 2 (doi:
671 10.5067/AXE4121732AD)
- 672 Nakayama Y, Manucharyan G, Zhang H, Dutrieux P, Torres HS, Klein P, Seroussi H, Schodlok M, Rignot E and
673 Menemenlis D (2019) Pathways of ocean heat towards Pine Island and Thwaites grounding lines. *Scientific Reports*,
674 **9**(1), ISSN 2045-2322 (doi: 10.1038/s41598-019-53190-6)
- 675 Nash D, Waliser D, Guan B, Ye H and Ralph FM (2018) The role of atmospheric rivers in extratropical and
676 polar hydroclimate. *Journal of Geophysical Research: Atmospheres*, **123**(13), 6804–6821, ISSN 2169-8996 (doi:
677 10.1029/2017jd028130)
- 678 Nicolas JP and Bromwich DH (2011) Climate of west Antarctica and influence of marine air intrusions*. *Journal of*
679 *Climate*, **24**(1), 49–67, ISSN 0894-8755 (doi: 10.1175/2010jcli3522.1)
- 680 Paolo FS, Fricker HA and Padman L (2015) Volume loss from Antarctic ice shelves is accelerating. *Science*, **348**(6232),
681 327–331, ISSN 1095-9203 (doi: 10.1126/science.aaa0940)
- 682 Park JY, Schloesser F, Timmermann A, Choudhury D, Lee JY and Nellikattil AB (2023) Future sea-level pro-
683 jections with a coupled atmosphere-ocean-ice-sheet model. *Nature Communications*, **14**(1), ISSN 2041-1723 (doi:
684 10.1038/s41467-023-36051-9)
- 685 Payne AE, Demory ME, Leung LR, Ramos AM, Shields CA, Rutz JJ, Siler N, Villarini G, Hall A and Ralph FM
686 (2020) Responses and impacts of atmospheric rivers to climate change. *Nature Reviews Earth and Environment*,
687 **1**(3), 143–157, ISSN 2662-138X (doi: 10.1038/s43017-020-0030-5)
- 688 Pollard D, DeConto RM and Alley RB (2015) Potential Antarctic ice sheet retreat driven by hydrofracturing and ice
689 cliff failure. *Earth and Planetary Science Letters*, **412**, 112–121, ISSN 0012-821X (doi: 10.1016/j.epsl.2014.12.035)
- 690 Rendfrey TS, Pettersen C, Bassis JN and Mateling ME (2024) CloudSat bservations show enhanced moisture trans-
691 port events increase snowfall rate and frequency over Antarctic Ice Sheet basins. *Journal of Geophysical Research:*
692 *Atmospheres*, **129**(6), e2023JD040556, ISSN 2169-8996 (doi: 10.1029/2023JD040556)

- 693 Rignot E (2002) Ice-shelf changes in Pine Island Bay, Antarctica, 1947–2000. *Journal of Glaciology*, **48**(161), 247–256,
694 ISSN 1727-5652 (doi: 10.3189/172756502781831386)
- 695 Rignot E, Mouginot J, Scheuchl B, van den Broeke M, van Wessem MJ and Morlighem M (2019) Four decades
696 of Antarctic Ice Sheet mass balance from 1979–2017. *Proceedings of the National Academy of Sciences*, **116**(4),
697 1095–1103, ISSN 1091-6490 (doi: 10.1073/pnas.1812883116)
- 698 Robel AA and Banwell AF (2019) A speed limit on ice shelf collapse through hydrofracture. *Geophysical Research*
699 *Letters*, **46**(21), 12092–12100, ISSN 1944-8007 (doi: 10.1029/2019gl084397)
- 700 Robin G de Q (1979) Formation, flow, and disintegration of ice shelves. *Journal of Glaciology*, **24**(90), 259–271, ISSN
701 1727-5652 (doi: 10.3189/s0022143000014787)
- 702 Scambos TA, Hulbe C, Fahnestock M and Bohlander J (2000) The link between climate warming and break-
703 up of ice shelves in the Antarctic peninsula. *Journal of Glaciology*, **46**(154), 516–530, ISSN 1727-5652 (doi:
704 10.3189/172756500781833043)
- 705 Schlemm T and Levermann A (2021) A simple parametrization of mélange buttressing for calving glaciers. *The*
706 *Cryosphere*, **15**(2), 531–545, ISSN 1994-0416 (doi: 10.5194/tc-15-531-2021), publisher: Copernicus GmbH
- 707 Sergienko OV (2010) Elastic response of floating glacier ice to impact of long-period ocean waves. *Journal of Geo-*
708 *physical Research: Earth Surface*, **115**(F4), ISSN 2156-2202 (doi: 10.1029/2010JF001721)
- 709 Shields CA, Wille JD, Marquardt Collow AB, MacLennan M and Gorodetskaya IV (2022) Evaluating uncertainty
710 and modes of variability for Antarctic atmospheric rivers. *Geophysical Research Letters*, **49**(16), ISSN 1944-8007
711 (doi: 10.1029/2022gl099577)
- 712 Swetha Chittella SP, Deb P and Melchior van Wessem J (2022) Relative contribution of atmospheric drivers to
713 “extreme” snowfall over the Amundsen Sea Embayment. *Geophysical Research Letters*, **49**(16), ISSN 1944-8007
714 (doi: 10.1029/2022gl098661)
- 715 Terpstra A, Gorodetskaya IV and Sodemann H (2021) Linking sub-tropical evaporation and extreme precipitation
716 over East Antarctica: An atmospheric river case study. *Journal of Geophysical Research: Atmospheres*, **126**(9),
717 ISSN 2169-8996 (doi: 10.1029/2020jd033617)
- 718 Trusel LD, Frey KE, Das SB, Munneke PK and van den Broeke MR (2013) Satellite-based estimates of
719 Antarctic surface meltwater fluxes. *Geophysical Research Letters*, **40**(23), 6148–6153, ISSN 1944-8007 (doi:
720 10.1002/2013gl058138)

- 721 Turton JV, Kirchgaessner A, Ross AN, King JC and Kuipers Munneke P (2020) The influence of föhn winds on
722 annual and seasonal surface melt on the Larsen C Ice Shelf, antarctica. *The Cryosphere*, **14**(11), 4165–4180, ISSN
723 1994-0424 (doi: 10.5194/tc-14-4165-2020)
- 724 van den Broeke M (2005) Strong surface melting preceded collapse of Antarctic Peninsula ice shelf. *Geophysical*
725 *Research Letters*, **32**(12), ISSN 1944-8007 (doi: 10.1029/2005gl023247)
- 726 van Wessem JM, van den Broeke MR, Wouters B and Lhermitte S (2023) Variable temperature thresholds of
727 melt pond formation on Antarctic ice shelves. *Nature Climate Change*, **13**(2), 161–166, ISSN 1758-6798 (doi:
728 10.1038/s41558-022-01577-1)
- 729 Walker CC, Bassis JN, Fricker HA and Czerwinski RJ (2013) Structural and environmental controls on Antarctic ice
730 shelf rift propagation inferred from satellite monitoring. *Journal of Geophysical Research: Earth Surface*, **118**(4),
731 2354–2364, ISSN 2169-9011 (doi: 10.1002/2013JF002742)
- 732 Walker CC, Bassis JN, Fricker HA and Czerwinski RJ (2015) Observations of interannual and spatial variability
733 in rift propagation in the Amery Ice Shelf, Antarctica, 2002–14. *Journal of Glaciology*, **61**(226), 243–252, ISSN
734 1727-5652 (doi: 10.3189/2015jog14j151)
- 735 Walker CC, Becker MK and Fricker HA (2021) A high resolution, three-dimensional view of the D-28 calving event
736 from Amery Ice Shelf with ICESat-2 and satellite imagery. *Geophysical Research Letters*, **48**(3), ISSN 1944-8007
737 (doi: 10.1029/2020gl091200)
- 738 Wilks DS (2011) *Statistical methods in the atmospheric sciences*. Academic press
- 739 Wille JD, Favier V, Dufour A, Gorodetskaya IV, Turner J, Agosta C and Codron F (2019) West Antarctic surface
740 melt triggered by atmospheric rivers. *Nature Geoscience*, **12**(11), 911–916, ISSN 1752-0908 (doi: 10.1038/s41561-
741 019-0460-1)
- 742 Wille JD, Favier V, Gorodetskaya IV, Agosta C, Kittel C, Beeman JC, Jourdain NC, Lenaerts JTM and Codron
743 F (2021) Antarctic atmospheric river climatology and precipitation impacts. *Journal of Geophysical Research:*
744 *Atmospheres*, **126**(8), ISSN 2169-8996 (doi: 10.1029/2020jd033788)
- 745 Wille JD, Favier V, Jourdain NC, Kittel C, Turton JV, Agosta C, Gorodetskaya IV, Picard G, Codron F, Santos
746 CLD, Amory C, Fettweis X, Blanchet J, Jomelli V and Berchet A (2022) Intense atmospheric rivers can weaken
747 ice shelf stability at the Antarctic Peninsula. *Communications Earth and Environment*, **3**(1), ISSN 2662-4435 (doi:
748 10.1038/s43247-022-00422-9)
- 749 Wille JD, Alexander SP, Amory C, Baiman R, Barthélemy L, Bergstrom DM, Berne A, Binder H, Blanchet J,
750 Bozkurt D, Bracegirdle TJ, Casado M, Choi T, Clem KR, Codron F, Datta R, Battista SD, Favier V, Francis D,

- 751 Fraser AD, Fourré E, Garreaud RD, Genthon C, Gorodetskaya IV, González-Herrero S, Heinrich VJ, Hubert G,
752 Joos H, Kim SJ, King JC, Kittel C, Landais A, Lazzara M, Leonard GH, Lieser JL, MacLennan M, Mikolajczyk D,
753 Neff P, Ollivier I, Picard G, Pohl B, Ralph FM, Rowe P, Schlosser E, Shields CA, Smith IJ, Sprenger M, Trusel L,
754 Udy D, Vance T, Vignon E, Walker C, Wever N and Zou X (2024) The extraordinary march 2022 east Antarctica
755 “heat” wave. part II: Impacts on the Antarctic ice sheet. *Journal of Climate*, **37**(3), 779–799, ISSN 1520-0442 (doi:
756 10.1175/jcli-d-23-0176.1)
- 757 Xiong X and Barnes W (2006) An overview of MODIS radiometric calibration and characterization. *Advances in*
758 *Atmospheric Sciences*, **23**(1), 69–79, ISSN 1861-9533 (doi: 10.1007/s00376-006-0008-3)